AIMS Mathematics, 9(3): 6513–6527.
DOI: 10.3934/math.2024317
Received: 12 September 2023
Revised: 09 December 2023
Accepted: 03 January 2024
Published: 06 February 2024

http://www.aimspress.com/journal/Math

Research article

Numerical simulation of Suliciu relaxation model via an mR scheme

Kamel Mohamed[1,2,*] **and Abdulhamed Alsisi**[1]

[1] Department of Mathematics, College of Science, Taibah University, Al-Madinah Al-Munawarah, Saudi Arabia

[2] Department of Mathematics, Faculty of Science, New Valley University, New Valley, Egypt

* **Correspondence:** Email: kmohamed@taibahu.edu.sa.

Abstract: We suggest a group of reliable and efficient finite volume techniques for solving the Suliciu relaxation model numerically. Namely, we have developed the modified Rusanov (mR) method to solve this model. This system is divided into two parts, the first of which is dependent on a local parameter that allows for diffusion control. The conservation equation is recovered in stage two. One of the key characteristics of the mR scheme is its ability to calculate the numerical flux equivalent to the solution's real state in the absence of the Riemann solution. Several numerical examples are considered. These examples indicate the mR scheme's high resolution and highlight its ability to deliver correct results for the Suliciu relaxation model. A variety of additional models in developed physics and applied science can be solved by using the mR method.

Keywords: conservation laws; Suliciu relaxation model; Riemann invariants; elementary waves; modified Rusanov scheme
Mathematics Subject Classification: 35L65, 35L67, 65M08, 65M12

1. Introduction

Hyperbolic conservation laws serve critical roles in the development of mathematical models for several natural processes in practical science. The form of the nonlinear systems of hyperbolic conservation laws is given by

$$\mathbb{W}_t + \mathrm{F}(\mathbb{W})_x = 0, \tag{1.1}$$

where $\mathbb{W} = (\mathbb{W}_1, ..., \mathbb{W}_n)$ and $\mathrm{F}(\mathbb{W}) = (\mathrm{F}_1(\mathbb{W}), ..., \mathrm{F}_n(\mathbb{W}))$ represent the conservative variable and physical flux respectively. The corresponding quasilinear system of system (1.1) is given by

$$\mathbb{W}_t + A(\mathbb{W})\mathbb{W}_x = 0, \quad A(\mathbb{W}) = F'(\mathbb{W}).$$

System (1.1) is strictly hyperbolic if the matrix $A(\mathbb{W})$ has n diverse real eigenvalues [1]:

$$\lambda_1 < \lambda_2 < ... < \lambda_n,$$

and n linearly independent corresponding right eigenvectors:

$$\gamma_1, \gamma_2, ..., \gamma_n.$$

Because conservation laws may have discontinuous solutions, they provide a significant theoretical and numerical problem [1, 2]. An i-characteristic field is genuinely nonlinear if

$$\nabla_{\mathbb{W}} \lambda_i(\mathbb{W}) \cdot \gamma_i(\mathbb{W}) \neq 0,$$

and linearly degenerate if the following holds:

$$\nabla_{\mathbb{W}} \lambda_i(\mathbb{W}) \cdot r_i(\mathbb{W}) = 0.$$

For a detailed discussion of the hyperbolic conservation law hypothesis, see [1–4]. The investigations of the initial value problems corresponding to Eq (1.1) produce very vital features in natural science, such as the shallow water model [5], Suliciu relaxation model [6], phonon-Bose model [7], Brio model [8], Chaplygin gas model [9] and many others. The highly significant conservation law is actually hidden behind a number of mathematical models [10, 11]. The development of numerical simulations has recently become one of the most important methods to better understand systems of hyperbolic conservation laws [12–15]. Nonlinear hyperbolic systems of coupled nonlinear equations may represent many flow fields including wave events. The Suliciu relaxation model is one of the most well known. This model has been extensively discussed due to its considerable physical basis and variety of useful applications [16–18].

Many applications depend on the modeling of viscoelastic materials and fluids. A viscoelastic fluid, specifically, is a material that, when deformed, demonstrates both viscous and elastic properties. Another significant feature of viscoelastic materials is that their mechanical characteristics are affected by the rate at which they are distorted. Viscoelastic fluids with significant applications include unset cement, gelatin, asphalt, latex paint, and many others [6]. The rheological reaction of such viscoelastic fluids can be quite complex. Recently, scholars have shown that model uncertainties can be evaluated by contrasting them with outcomes from tests and in-service experiences, or with other, more sophisticated approaches [19, 20]. When a decision-maker believes that the model that they are using is an approximation of the "correct" reference model rather than the ideal means of describing the future states of the world, model uncertainty elements are introduced.

In the ongoing research, we are developing the modified Rusanov (mR) method to solve the Suliciu relaxation model in one dimension of space. This strategy has stages for predictors and correctors [21–27]. The numerical diffusion control parameter in the first stage is based on the theory of Riemann invariants and limiters. The balanced conservation equation is recovered in the second stage. The scheme's stability analysis indicates that the scheme's order is determined by the value of the control parameter [27]. In most common schemes, Riemann solutions were used to calculate the numerical flux. The numerical flux was calculated by using Riemann solutions in the majority of typical schemes. In contrast to earlier schemes, the mR scheme has the intriguing ability of evaluating

the numerical flux in the absence of the Riemann solution. This scheme, in fact, can be used as a box solver for many different conservation law models.

The structure of the article is as follows. Section 2 introduces the mathematical Suliciu relaxation model. Section 3 presents the structure of the mR technique to solve the 1D Suliciu relaxation model. Section 4 includes numerous numerical test cases to investigate the wave creation processes. Conclusions and observations about the current results are presented in Section 5.

2. Mathematical model

The Suliciu relaxation model [6,16–18,28] clarifies the following information about the viscoelastic shallow fluid:

$$\begin{aligned} &\frac{\partial \rho}{\partial t} + \frac{\partial \rho u}{\partial x} = 0, \\ &\frac{\partial \rho u}{\partial t} + \frac{\partial (\rho u^2 + s^2 v)}{\partial x} = 0, \\ &\frac{\partial \rho v}{\partial t} + \frac{\partial (\rho u v + u)}{\partial x} = 0\,, \end{aligned} \tag{2.1}$$

where $\rho \geq 0$ displays the fluid's layer depth, u is the horizontal speed, $s > 0$ is associated with the stress tensor, $v = \frac{\pi}{s^2}$ is the new parameter related to pressure, and π represents the relaxed pressure. As a relaxation for the isentropic Chaplygin gas dynamics system, the following model can be utilized [29, 30]:

$$\begin{aligned} &\frac{\partial \rho}{\partial t} + \frac{\partial \rho u}{\partial x} = 0, \\ &\frac{\partial \rho u}{\partial t} + \frac{\partial (\rho u^2 + P)}{\partial x} = 0, \end{aligned} \tag{2.2}$$

where $\rho > 0$ represents the density of the gas u represents the speed, and the state equation gives the pressure $P = -\frac{s^2}{\rho}$ with the constant $s > 0$. We rewrite system (2.1) as follows:

$$\frac{\partial \mathbb{W}}{\partial t} + \frac{\partial \mathrm{F}}{\partial x} = 0, \tag{2.3}$$

$$\mathbb{W} = \begin{pmatrix} \rho \\ \rho u \\ \rho v \end{pmatrix}, \qquad \mathrm{F}(\mathbb{W}) = \begin{pmatrix} \rho u \\ \rho u^2 + s^2 v \\ \rho u v + u \end{pmatrix}.$$

System (2.1) is strictly hyperbolic since it has the following eigenvalues:

$$\lambda_1 = u - \frac{s}{\rho}, \;\; \lambda_2 = u, \;\; \lambda_3 = u + \frac{s}{\rho}. \tag{2.4}$$

The eigenvectors of system (2.1) are

$$\gamma_1 = \left(\rho^2, -s, 1\right)^T, \;\; \gamma_2 = (1, 0, 0)^T, \;\; \gamma_3 = \left(\rho^2, s, 1\right)^T.$$

System (2.1) is linearly degenerate because $\nabla\lambda_1 \cdot \gamma_1 = \nabla\lambda_2 \cdot \gamma_2 = \nabla\lambda_3 \cdot \gamma_3 = 0$. The corresponding Riemann invariants are given by

$$R_1 = s^2\, v - s\, u, \;\; R_2 = v + \frac{1}{\rho}, \;\; R_3 = s^2\, v + s\, u. \tag{2.5}$$

3. The mR scheme

Here, we describe the mR scheme by integrating Eq (2.3) over the domain $[t_n, t_{n+1}] \times [x_{i-\frac{1}{2}}, x_{i+\frac{1}{2}}]$, given as follows:

$$\mathbb{W}_i^{n+1} = \mathbb{W}_i^n - \frac{\Delta t}{\Delta x}\left(\mathrm{F}\left(\mathbb{W}_{i+\frac{1}{2}}^n\right) - \mathrm{F}\left(\mathbb{W}_{i-\frac{1}{2}}^n\right)\right), \tag{3.1}$$

where $\mathbb{W}_i^n$ is the solution's average of $\mathbb{W}$ over the interval $[x_{i-\frac{1}{2}}, x_{i+\frac{1}{2}}]$ at time t_n, i.e.,

$$\mathbb{W}_i^n = \frac{1}{\Delta x}\int_{x_{i-\frac{1}{2}}}^{x_{i+\frac{1}{2}}} \mathbb{W}(t_n, x)\, dx,$$

where $\mathrm{F}(\mathbb{W}_{i\pm\frac{1}{2}}^n)$ denotes the numerical flux at time t_n and given a space $x = x_{i\pm\frac{1}{2}}$. In order to construct the numerical fluxes, $\mathrm{F}\left(\mathbb{W}_{i\pm\frac{1}{2}}^n\right)$ in the finite volume discretization given by Eq (3.1), Riemann problems at the cell interfaces $x_{i\pm\frac{1}{2}}$ must be solved. According to the following initial condition, we assume that the self-similar solution to the Riemann problem associated with Eq (2.3) exists:

$$\mathbb{W}(x, 0) = \begin{cases} \mathbb{W}_L, & \text{if} \quad x < 0, \\ \mathbb{W}_R, & \text{if} \quad x > 0, \end{cases} \tag{3.2}$$

and it is provided by

$$\mathbb{W}(t, x) = R_s\left(\frac{x}{t}, \mathbb{W}_L, \mathbb{W}_R\right),$$

where R_s denotes the Riemann solution, which must be calculated precisely or approximated. Thus, at the cell interface $x = x_{i\pm\frac{1}{2}}$, the intermediate state $\mathbb{W}_{i\pm\frac{1}{2}}^n$ in Eq (3.1) is defined as follows:

$$\mathbb{W}_{i+\frac{1}{2}}^n = R_s\left(0, \mathbb{W}_i^n, \mathbb{W}_{i+1}^n\right). \tag{3.3}$$

From a computational viewpoint, the process is very demanding and may limit the use of the scheme for which Riemann solutions are challenging to approximate. In order to get around these numerical challenges and approximate $\mathbb{W}_{i+\frac{1}{2}}^n$, we modify a Rusanov scheme that was proposed in [21–26]. In order to create $\mathbb{W}_{i+\frac{1}{2}}^n$ for use in the corrector step given by Eq (3.1), we integrate Eq (2.3) over the domain $[t_n, t_n + \theta_{i+\frac{1}{2}}^n] \times [x^-, x^+]$; see Figure 1. Here, $\mathbb{W}_{i\pm\frac{1}{2}}^n$ is an approximation of the Riemann solution R_s based on the control volume $[x^-, x^+]$ at $t_n + \theta_{i+\frac{1}{2}}^n$. Consequently, we arrive at the intermediate state as follows:

$$\int_{x^-}^{x^+} \mathbb{W}(t_n + \theta_{i+\frac{1}{2}}^n, x)\, dx = \Delta x^- \mathbb{W}_i^n + \Delta x^+ \mathbb{W}_{i+1}^n - \theta_{i+\frac{1}{2}}^n\Big(\mathrm{F}(\mathbb{W}_{i+1}^n) - \mathrm{F}(\mathbb{W}_i^n)\Big), \tag{3.4}$$

where the distance measures Δx^- and Δx^+ are given by

$$\Delta x^- = \left|x^- - x_{i+\frac{1}{2}}\right|, \qquad \Delta x^+ = \left|x^+ - x_{i+\frac{1}{2}}\right|.$$

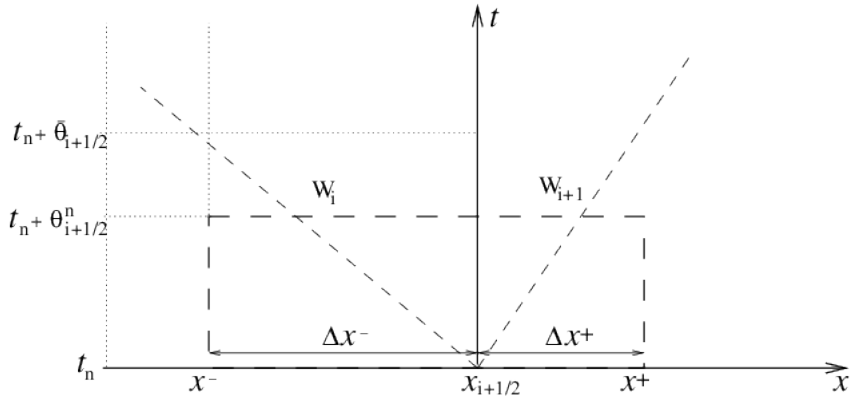

Figure 1. The control volume depicting the mR scheme.

If we set $x^- = x_i$ and $x^+ = x_{i+1}$ in Eq (3.4), then the predictor stage is given by

$$\mathbb{W}^n_{i+\frac{1}{2}} = \frac{1}{2}\left(\mathbb{W}^n_i + \mathbb{W}^n_{i+1}\right) - \frac{\theta^n_{i+\frac{1}{2}}}{\Delta x}\Big(\mathrm{F}(\mathbb{W}^n_{i+1}) - \mathrm{F}(\mathbb{W}^n_i)\Big), \tag{3.5}$$

where $\mathbb{W}^n_{i+\frac{1}{2}}$ is the solution's average of $\mathbb{W}$ over the interval $[t_n, t_n + \theta^n_{i+\frac{1}{2}}] \times [x_i, x_{i+1}]$ and is described as

$$\mathbb{W}^n_{i+\frac{1}{2}} = \frac{1}{\Delta x}\int_{x_i}^{x_{i+1}} \mathbb{W}(x, t_n + \theta^n_{i+\frac{1}{2}})dx. \tag{3.6}$$

The parameter $\theta^n_{i+\frac{1}{2}}$ must be chosen to complete the implementation of the proposed finite volume scheme; the choice of the parameter $\theta^n_{i+\frac{1}{2}}$ depends on the stability analysis scheme; for more information, see [21]; we choose the variable $\theta^n_{i+\frac{1}{2}}$ as follows:

$$\theta^n_{i+\frac{1}{2}} = \alpha^n_{i+\frac{1}{2}}\frac{\Delta x}{2S^n_{i+\frac{1}{2}}}, \tag{3.7}$$

where $\alpha^n_{i+\frac{1}{2}}$ is a local parameter that needs to be determined locally, and $S^n_{i+\frac{1}{2}}$ is the local Rusanov velocity defined as

$$S^n_{i+\frac{1}{2}} = \max_{k=1,\ldots,K}(\max(|\,\lambda^n_{k,i}\,|, |\,\lambda^n_{k,i+1}\,|)), \tag{3.8}$$

where $\lambda^n_{k,i}$ denotes the k-th eigenvalues in Eq (2.4). The predictor stage defined in Eq (3.5) can then be rewritten.

$$\mathbb{W}^n_{i+\frac{1}{2}} = \frac{1}{2}(\mathbb{W}^n_i + \mathbb{W}^n_{i+1}) - \frac{\alpha^n_{i+\frac{1}{2}}}{2S^n_{j+\frac{1}{2}}}\left[\mathrm{F}(\mathbb{W}^n_{i+1}) - \mathrm{F}(\mathbb{W}^n_i)\right]. \tag{3.9}$$

It is clear that when $\alpha^n_{i+\frac{1}{2}} = \frac{\Delta t}{\Delta x}S^n_{j+\frac{1}{2}}$ the Lax-Wendroff method is reduced to the proposed finite volume scheme [2]; also, when $\alpha^n_{i+\frac{1}{2}} = 1$ in the linear case, the proposed scheme is reduced to the upwind scheme. Another option for the slopes is that $\alpha^n_{i+\frac{1}{2}}$ can be written as

$$\alpha^n_{i+\frac{1}{2}} = \left(1 - \Phi\left(\mathrm{r}_{i+\frac{1}{2}}\right)\right)\frac{S^n_{i+\frac{1}{2}}}{s^n_{i+\frac{1}{2}}} + \frac{\Delta t}{\Delta x}S^n_{i+\frac{1}{2}}\Phi\left(\mathrm{r}_{i+\frac{1}{2}}\right), \tag{3.10}$$

where $s^n_{i+\frac{1}{2}} = \min\limits_{k=1,\dots,K}(\max(|\ \lambda^n_{k,i}\ |,|\ \lambda^n_{k,i+1}\ |))$, $\Phi_{i+\frac{1}{2}} = \Phi\left(\mathrm{r}_{i+\frac{1}{2}}\right)$ is a suitable limiter that is determined by a flux limiter function Φ acting on a quantity that measures the ratio $\mathrm{r}_{i+\frac{1}{2}} = \frac{\mathbb{W}_{i+1-q}-\mathbb{W}_{i-q}}{\mathbb{W}_{i+1}-\mathbb{W}_i}$ and $q = \mathrm{sign}\left[\mathrm{F}'(\mathbb{W}^n_{i+\frac{1}{2}})\right]$ of the upwind change to the local position through the use of the Riemann invariants defined in Eq (2.5), see for instance [31]. Here, the minmod function is defined by

$$\Phi(\mathrm{r}) = \max\left(0, \min\left(1, \mathrm{r}\right)\right), \tag{3.11}$$

and the van Albada function

$$\Phi(\mathrm{r}) = \frac{\mathrm{r} + \mathrm{r}^2}{1 + \mathrm{r}^2} \tag{3.12}$$

are used; see [2, 32] for the limiter functions that allow for the use of van Leer or superbee functions. The mR scheme for Eq (2.3) is finally written as follows:

$$\begin{cases} \mathbb{W}^n_{i+\frac{1}{2}} = \dfrac{1}{2}(\mathbb{W}^n_i + \mathbb{W}^n_{i+1}) - \dfrac{\alpha^n_{i+\frac{1}{2}}}{2S^n_{j+\frac{1}{2}}}\left[\mathrm{F}(\mathbb{W}^n_{i+1}) - \mathrm{F}(\mathbb{W}^n_i)\right], \\ \mathbb{W}^{n+1}_i = \mathbb{W}^n_i - r^n\left[\mathrm{F}\left(\mathbb{W}^n_{i+\frac{1}{2}}\right) - \mathrm{F}\left(\mathbb{W}^n_{i-\frac{1}{2}}\right)\right]. \end{cases} \tag{3.13}$$

4. Numerical results

We introduce six numerical test cases through the use of the mR, Rusanov, Lax-Friedrichs, and Harten-Lax-van Leer (HLL) schemes for numerical simulation of the suliciu relaxation system. We show the accuracy of the proposed mR method. For all computations the domain is $[-1, 1]$, whereas we discretize with 200 grid points and the final time is $t = 0.1s$. We compare the results of the three schemes with the reference solution obtained via the classical Rusanov scheme on the very fine mesh of 20000 grid points. We chose the condition of stability [21] as follows:

$$\Delta t = CFL\frac{\Delta x}{\max\limits_i(\left|\alpha^n_{i+\frac{1}{2}} S^n_{i+\frac{1}{2}}\right|)}, \tag{4.1}$$

where $CFL = 0.9$ in all test cases, except test case 4, where we take it as 0.5.

4.1. Test case 1

In this test case, while the solution is represented by a delta shock and a rarefaction wave moving from left to right in Figures 2 and 3, we take into consideration the following initial conditions:

$$(\rho, u, v) = \begin{cases} (9, 5, \frac{14}{5}), & \text{if} \quad x \le 0, \\ (1, 3, 2), & \text{if} \quad x \ge 0. \end{cases} \tag{4.2}$$

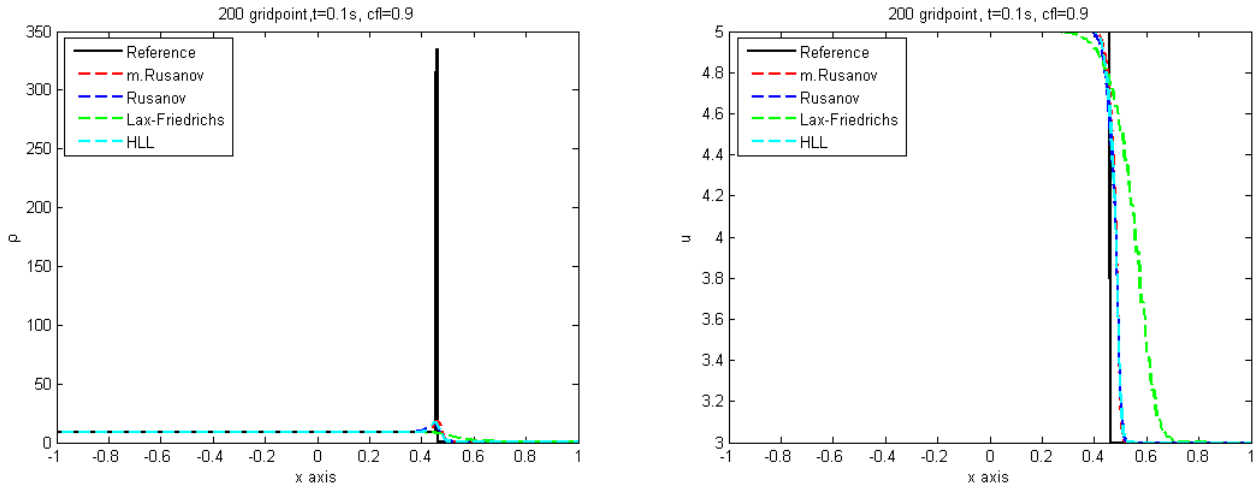

Figure 2. Density ρ (left) and u (right).

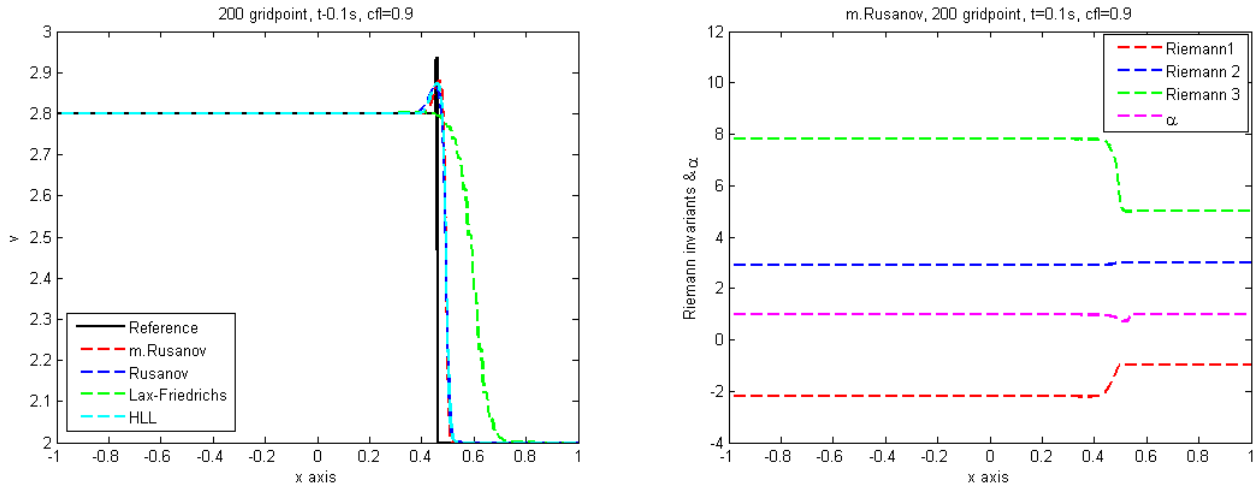

Figure 3. Velocity v (left) and α^n and Riemann invariants (right).

4.2. Test case 2

In this test case, while the solution is represented by a rarefaction and shock wave continuing from left to right in Figures 4 and 5, we take into consideration the following initial conditions:

$$(\rho, u, v) = \begin{cases} (7, 2, 2), & \text{if} \quad x \leq 0, \\ (5, 7, 2), & \text{if} \quad x \geq 0. \end{cases} \tag{4.3}$$

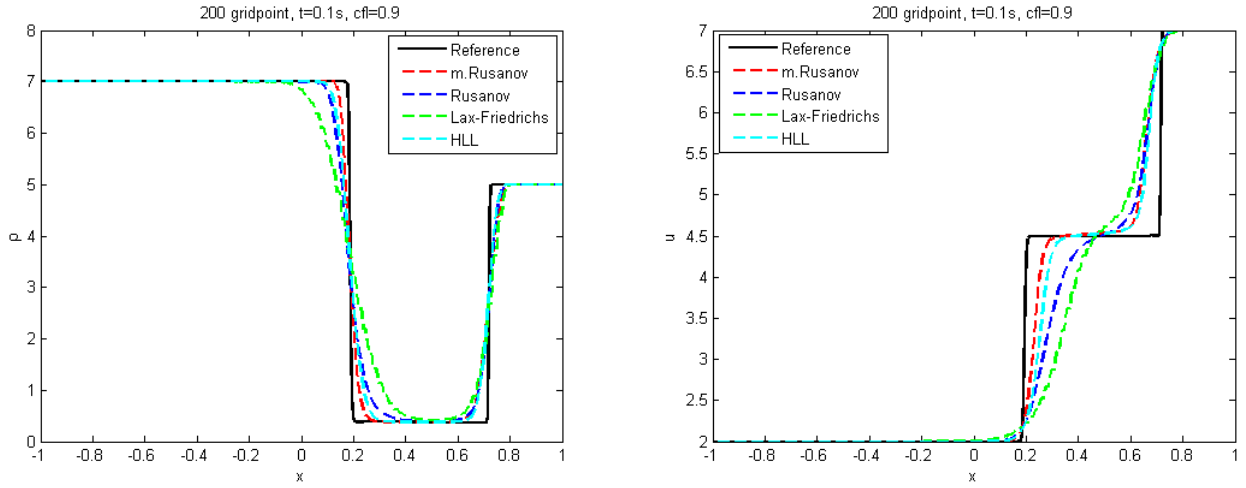

Figure 4. Density ρ (left) and u (right).

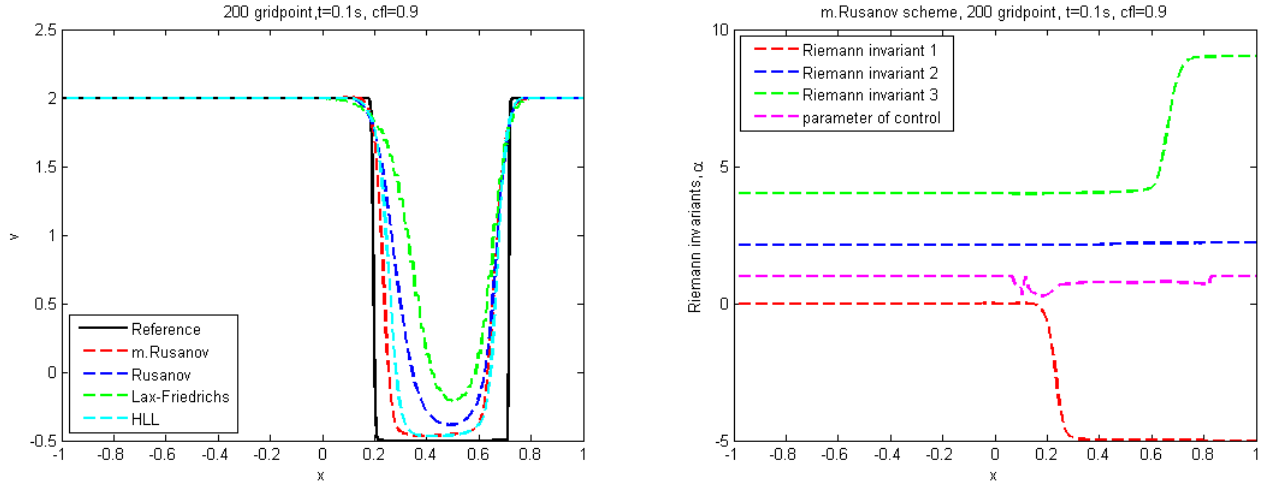

Figure 5. Velocity v (left) and α^n and Riemann invariants (right).

4.3. Test case 3

In this test case, the solution consists of a shock wave proceeding from left to right and a rarefaction continuing from right to left; see Figures 6 and 7, where the initial conditions are as follows:

$$(\rho, u, v) = \begin{cases} (1, 0, 1), & \text{if} \quad x \leq 0, \\ (0.25, 0, 0), & \text{if} \quad x \geq 0. \end{cases} \tag{4.4}$$

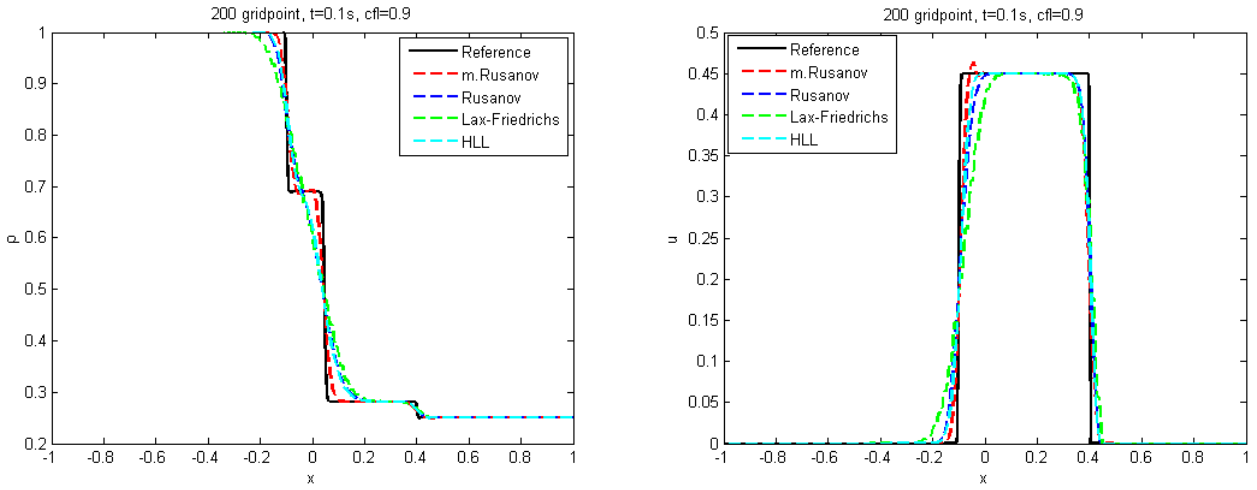

Figure 6. Density ρ (left) and u (right).

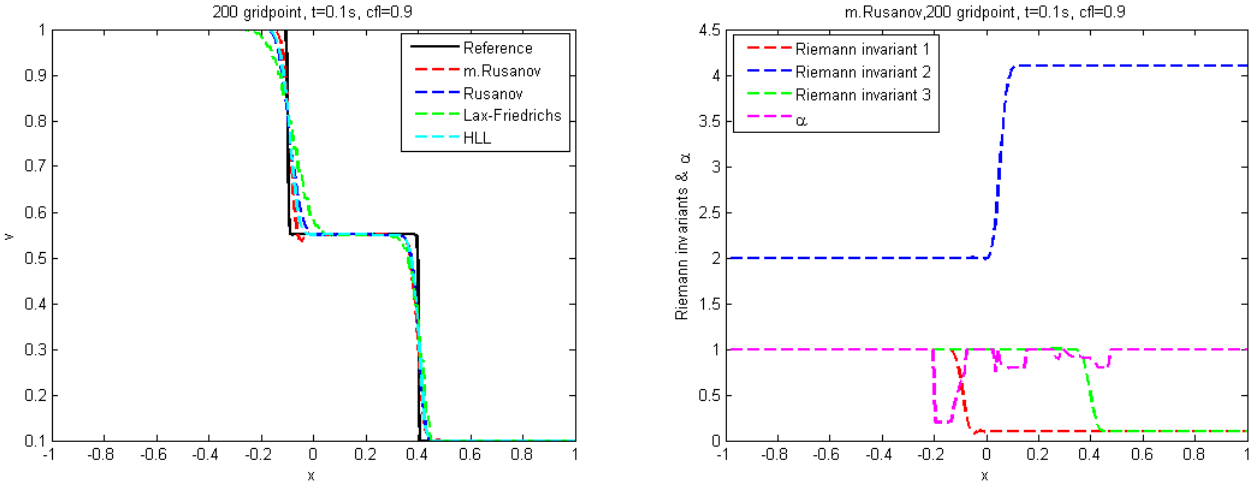

Figure 7. Velocity v (left) and α^n and Riemann invariants (right).

4.4. Test case 4

In this test case, while the solution is a pair of rarefaction waves traveling from left to right, we take into consideration the following starting points; see Figures 8 and 9.

$$(\rho, u, v) = \begin{cases} (1, 3, 0.5), & \text{if} \quad x \leq 0, \\ (1.5, 3, 2), & \text{if} \quad x \geq 0. \end{cases} \tag{4.5}$$

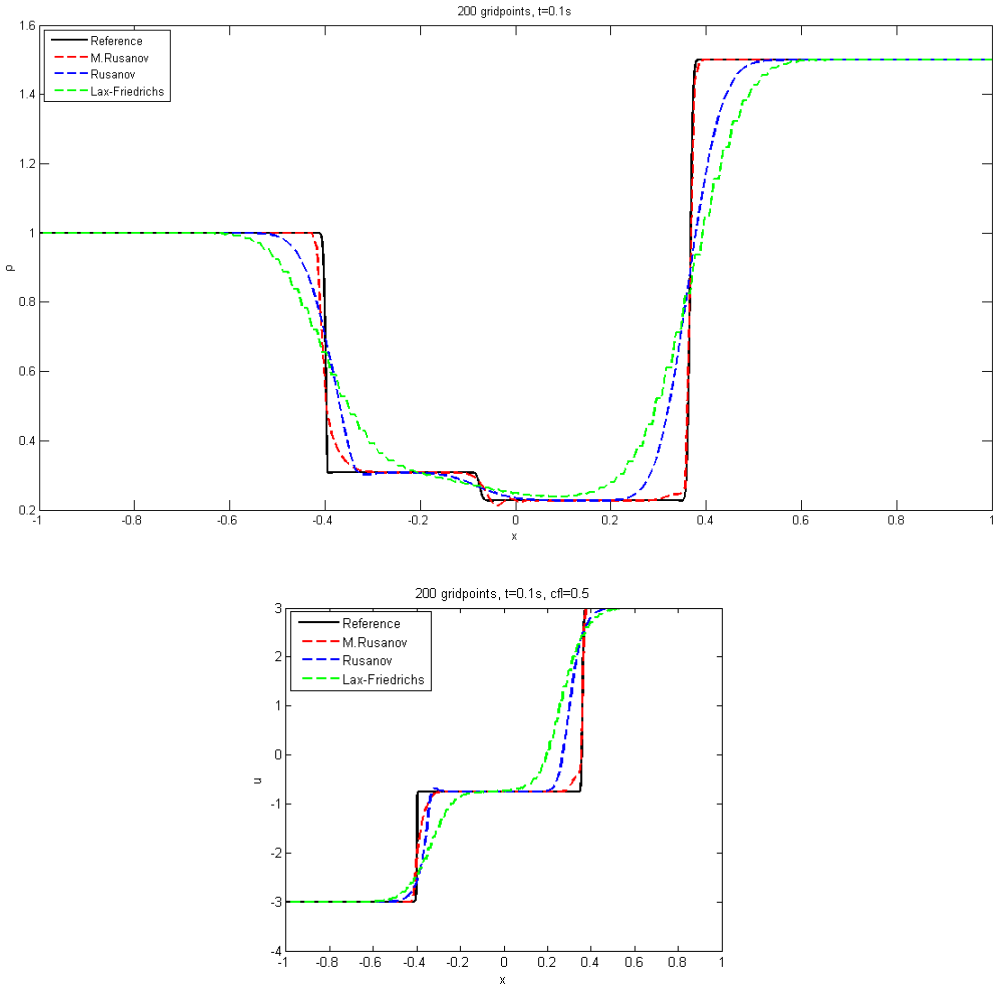

Figure 8. Density ρ (upper) and u (lower).

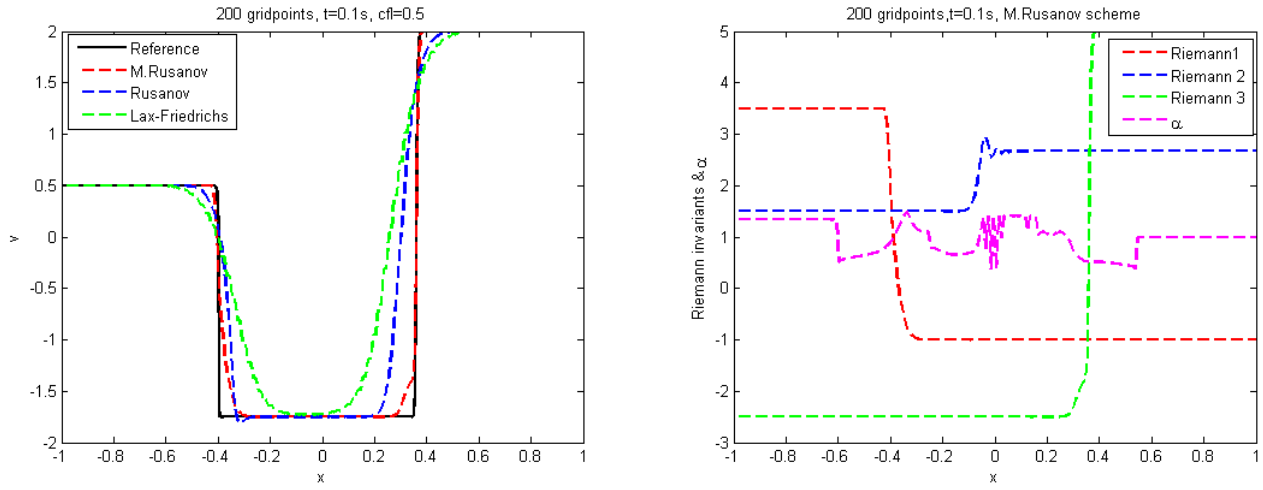

Figure 9. Velocity u (left) and α^n and Riemann invariants (right).

4.5. *Test case 5*

In this test case, we consider the following initial conditions, while the solution consists of a rarefaction wave and shock wave; see Figures 10 and 11.

$$(\rho, u, v) = \begin{cases} (0.5, 2, 1), & \text{if} \quad x \leq 0, \\ (0.6, 0, 1), & \text{if} \quad x \geq 0. \end{cases} \tag{4.6}$$

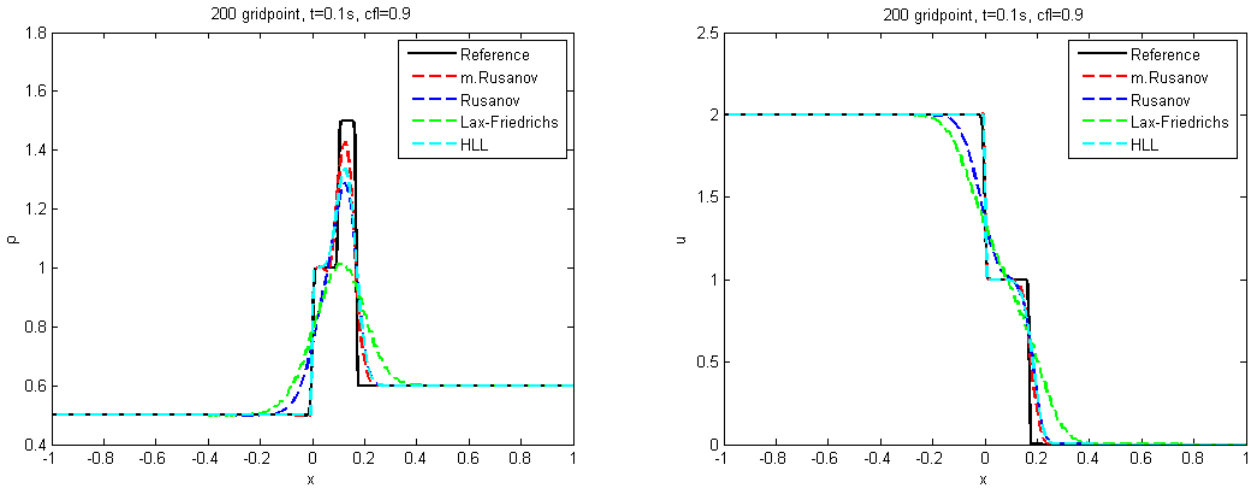

Figure 10. Density ρ (left) and u (right).

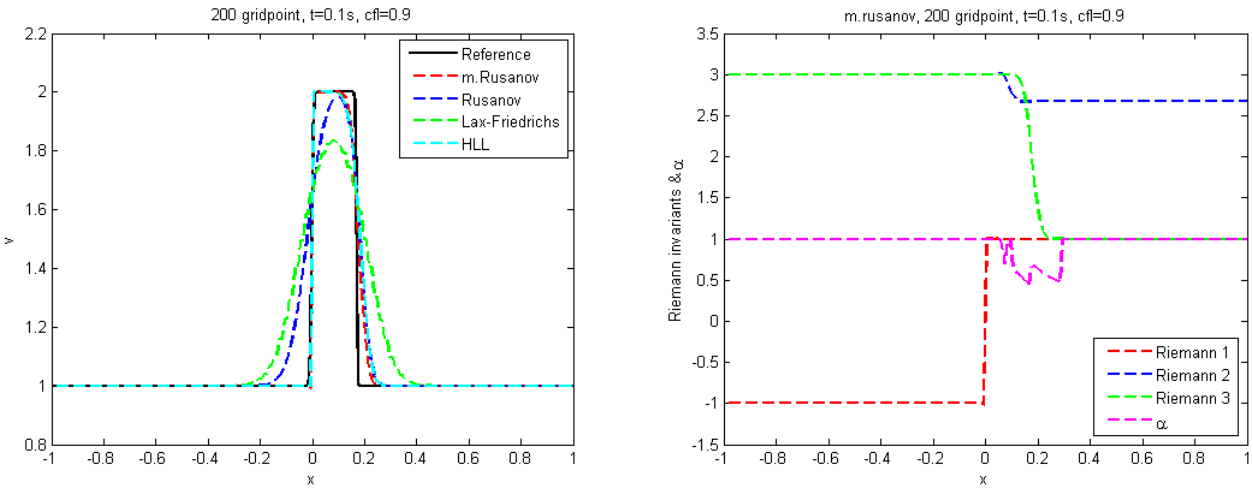

Figure 11. Velocity v (left) and α^n and Riemann invariants (right).

4.6. *Test case 6*

In this test case, the solution consists of a rarefaction wave and shock wave, as shown in Figures 12 and 13, where the initial conditions are as follows:

$$(\rho, u, v) = \begin{cases} (0.3, 0, 0.6), & \text{if} \quad x \leq 0, \\ (0.6, 0, 0.3), & \text{if} \quad x \geq 0. \end{cases} \tag{4.7}$$

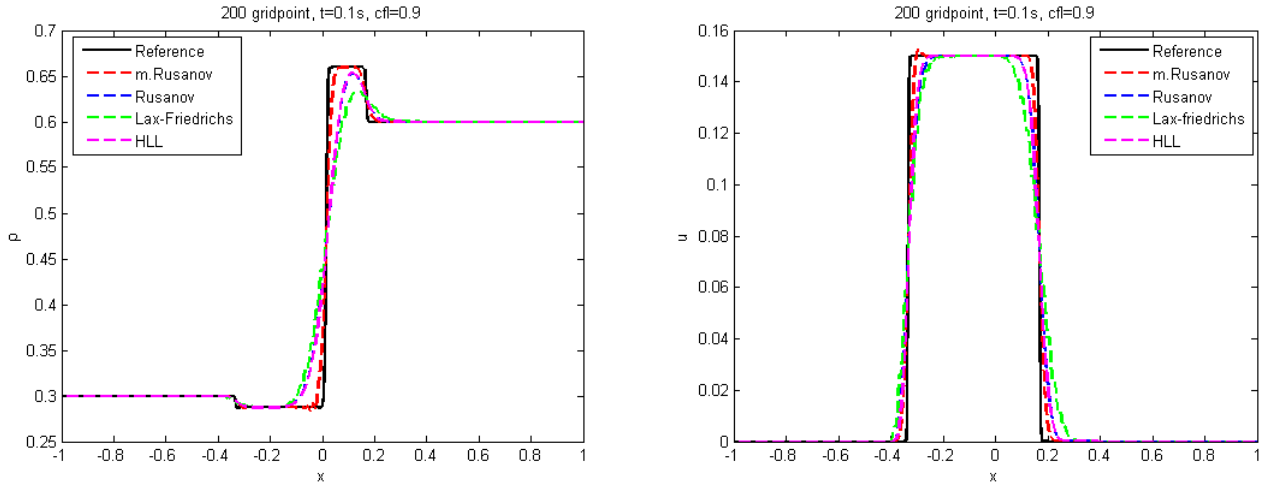

Figure 12. Density ρ (left) and u (right).

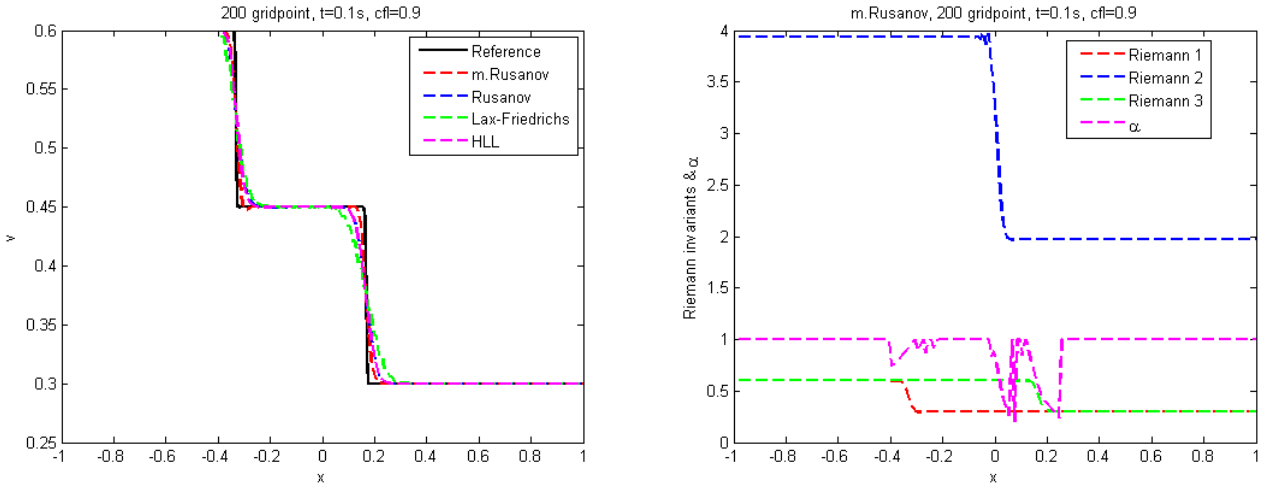

Figure 13. Velocity v (left) and α^n and Riemann invariants (right).

In summary, we have reported six numerical test cases corresponding to the Suliciu relaxation model. We noticed that the mR scheme is more accurate than the Rusanov scheme, HLL scheme and Lax-Friedrichs schemes. We compared these schemes with the reference solution on the very fine mesh of 20000 grid points. The accuracy of the HLL scheme is better than that of the Rusanov scheme

and Lax-Friedrichs scheme. Indeed, the presented four schemes are able to capture the rarefaction and shock waves.

5. Conclusions

The mR scheme was implemented to solve 1D Suliciu relaxation model. This scheme is capable of precisely capturing non-continuous profiles of hyperbolic systems of conservation laws and avoiding numerical diffusion in the solution. Various numerical examples have been provided to solve the Suliciu relaxation model through the use of the mR, Rusanov, Lax-Friedrichs, and HLL methods, as well as analytical solutions. The results demonstrate that the mR scheme offers remarkable shock resolution with high precision in the smooth zone and that there are no nonphysical oscillations around the shock locations. The simulations presented demonstrated the excellent resolution of the mR technique and confirmed its capabilities and effectiveness in dealing with such models.

Use of AI tools declaration

The authors declare that they have not used artificial intelligence tools in the creation of this article.

Acknowledgments

The authors extend their appreciation to the Deputyship for Research & Innovation, Ministry of Education in Saudi Arabia for funding this research work through the project number 445-9-582.

Conflict of interest

The authors declare that they have no competing interests.

References

1. J. Smoller, *Shock waves and reaction-diffusion equations*, New York: Springer, 1994. https://doi.org/10.1007/978-1-4612-0873-0
2. R. J. LeVeque, *Numerical methods for conservation laws*, Basel: Birkhäuser, 1990. https://doi.org/10.1007/978-3-0348-5116-9
3. L. C. Evans, *Partial differential equations*, American Mathematical Society, 1998.
4. E. F. Toro, *Riemann solvers and numerical methods for fluid dynamics*, Berlin, Heidelberg: Springer, 1997. https://doi.org/10.1007/978-3-662-03490-3
5. M. A. E. Abdelrahman, On the shallow water equations, *Z. Naturforsch. A*, **72** (2017), 873–879. https://doi.org/10.1515/zna-2017-0146
6. Y. Y. Zhang, Y. Zhang, The Riemann problem for the Suliciu relaxation system with the double-coefficient Coulomb-like friction terms, *Int. J. Non-Linear Mech.*, **116** (2019), 200–210. https://doi.org/10.1016/j.ijnonlinmec.2019.07.004

7. M. A. E. Abdelrahman, Cone-grid scheme for solving hyperbolic systems of conservation laws and one application, *Comput. Appl. Math.*, **37** (2018), 3503–3513. https://doi.org/10.1007/s40314-017-0527-9
8. H. Kalisch, V. Teyekpiti, Hydraulic jumps on shear flows with constant vorticity, *Eur. J. Mech. B/Fluids*, **72** (2018), 594–600. https://doi.org/10.1016/j.euromechflu.2018.08.005
9. K. Mohamed, H. A. Alkhidhr, M. A. E. Abdelrahman, The NHRS scheme for the Chaplygin gas model in one and two dimensions, *AIMS Math.*, **7** (2022), 17785–17801. https://doi.org/10.3934/math.2022979
10. S. Frassu, G. Viglialoro, Boundedness in a chemotaxis system with consumed chemoattractant and produced chemorepellent, *Nonlinear Anal.*, **213** (2021), 112505. https://doi.org/10.1016/j.na.2021.112505
11. T. X. Li, N. Pintus, G. Viglialoro, Properties of solutions to porous medium problems with different sources and boundary conditions, *Z. Angew. Math. Phys.*, **70** (2019), 86. https://doi.org/10.1007/s00033-019-1130-2
12. J. Britton, Y. L. Xing, High order still-water and moving-water equilibria preserving discontinuous Galerkin methods for the Ripa model, *J. Sci. Comput.*, **82** (2020), 30. https://doi.org/10.1007/s10915-020-01134-y
13. K. Mohamed, M. A. E. Abdelrahman, The NHRS scheme for the two models of traffic flow, *Comput. Appl. Math.*, **42** (2023), 53. https://doi.org/10.1007/s40314-022-02172-y
14. A. Rehman, I. Ali, S. Zia, S. Qamar, Well-balanced finite volume multi-resolution schemes for solving the Ripa models, *Adv. Mech. Eng.*, **13** (2021), 1–16. https://doi.org/10.1177/16878140211003418
15. K. Mohamed, M. A. E. Abdelrahman, The modified Rusanov scheme for solving the ultra-relativistic Euler equations, *Eur. J. Mech. B/Fluids*, **90** (2021), 89–98. https://doi.org/10.1016/j.euromechflu.2021.07.014
16. F. Bouchut, S. Boyaval, A new model for shallow viscoelastic fluids, *Math. Models Methods Appl. Sci.*, **23** (2013), 1479–1526. https://doi.org/10.1142/S0218202513500140
17. I. Suliciu, On modelling phase transitions by means of rate-type constitutive equations. Shock wave structure, *Int. J. Eng. Sci.*, **28** (1990), 829–841. https://doi.org/10.1016/0020-7225(90)90028-H
18. R. De la Cruz, J. Galvis, J. C. Juajibioy, L. Rendon, Delta shock wave for the Suliciu relaxation system, *Adv. Math. Phys.*, **2014** (2014), 1–11. https://doi.org/10.1155/2014/35434920
19. T. Jin, Y. G. Zhu, Y. D. Shu, J. Cao, H. Y. Yan, D. P. Jiang, Uncertain optimal control problem with the first hitting time objective and application to a portfolio selection model, *J. Intell. Fuzzy Syst.*, **44** (2023), 1585–1599. https://doi.org/10.3233/jifs-222041
20. T. Jin, F. Z. Li, H. J. Peng, B. Li, D. P. Jiang, Uncertain barrier swaption pricing problem based on the fractional differential equation in Caputo sense, *Soft Comput.*, **27** (2023), 11587–11602. https://doi.org/10.1007/s00500-023-08153-5
21. K. Mohamed, *Simulation numérique en volume finis, de problémes d'écoulements multidimensionnels raides, par un schéma de flux á deux pas*, University of Paris 13, 2005.

22. K. Mohamed, M. Seaid, M. Zahri, A finite volume method for scalar conservation laws with stochastic time-space dependent flux function, *J. Comput. Appl. Math.*, **237** (2013), 614–632. https://doi.org/10.1016/j.cam.2012.07.014

23. K. Mohamed, F. Benkhaldoun, A modified Rusanov scheme for shallow water equations with topography and two phase flows, *Eur. Phys. J. Plus*, **131** (2016), 207. https://doi.org/10.1140/epjp/i2016-16207-3

24. K. Mohamed, A finite volume method for numerical simulation of shallow water models with porosity, *Comput. Fluids*, **104** (2014), 9–19. https://doi.org/10.1016/j.compfluid.2014.07.020

25. K. Mohamed, S. Sahmim, F. Benkhaldoun, M. A. E. Abdelrahman, Some recent finite volume schemes for one and two layers shallow water equations with variable density, *Math. Methods Appl. Sci.*, **46** (2023), 12979–12995. https://doi.org/10.1002/mma.9227

26. M. A. E. Abdelrahman, H. A. Alkhidhr, K. Mohamed, Simulating isothermal Euler model with non-vacuum initial data via mR scheme, *J. Low Freq. Noise Vibration Active Control*, **41** (2022), 1466–1477. https://doi.org/10.1177/14613484221105147

27. K. Mohamed, S. Sahmim, M. A. E. Abdelrahman, A predictor-corrector scheme for simulation of two-phase granular flows over a moved bed with a variable topography, *Eur. J. Mech. B/Fluids*, **96** (2022), 39–50. https://doi.org/10.1016/j.euromechflu.2022.07.001

28. G. Carbou, B. Hanouzet, R. Natalini, Semilinear behavior for totally linearly degenerate hyperbolic systems with relaxation, *J. Differ. Equ.*, **246** (2009), 291–319. https://doi.org/10.1016/j.jde.2008.05.015

29. T. T. Chen, A. F. Qu, Z. Wang, The two-dimensional Riemann problem for isentropic Chaplygin gas, *Acta Math. Sci. Ser. A*, **37** (2017), 1053–1061.

30. Q. Wang, J. Q. Zhang, H. C. Yang, Two dimensional Riemann-type problem and shock diffraction for the Chaplygin gas, *Appl. Math. Lett.*, **101** (2020), 106046. https://doi.org/10.1016/j.aml.2019.106046

31. P. K. Sweby, High resolution schemes using flux limiters for hyperbolic conservation laws, *SIAM J. Numer. Anal.*, **21** (1984), 995–1011.

32. B. van Leer, Towards the ultimate conservative difference schemes. V. A second-order Ssequal to Godunov's method, *J. Comput. Phys.*, **32** (1979), 101–136. https://doi.org/10.1016/0021-9991(79)90145-1

AIMS Press